ELSEVIER

Journal of Alloys and Compounds 404–406 (2005) 307–311

Journal of ALLOYS AND COMPOUNDS

www.elsevier.com/locate/jallcom

# Miss MaRPel – a 3 MV pelletron accelerator for hydrogen depth profiling

M. Uhrmacher*, M. Schwickert, H. Schebela, K.-P. Lieb

*II. Physikalisches Institut, Universität Göttingen, Friedrich-Hund-Platz 1, D-37077 Göttingen, Germany*

Received 1 June 2004; accepted 8 September 2004
Available online 6 July 2005

**Abstract**

The 3 MV Pelletron tandem accelerator MaRPel (Material Research Pelletron) of the II. Physikalisches Institut in Göttingen is equipped with a low-level target station for applying the Resonant Nuclear Reaction Analysis technique. This combination allows high-resolution hydrogen depth distribution profiling using a $^{15}$N beam with an energy higher than 6.385 MeV, which is the resonance energy of the $^{1}$H($^{15}$N, $\alpha\gamma$)$^{12}$C nuclear reaction. The installed AMSEL-steerers are used for an easy variation of the beam energy and a computer-controlled automated measurement of depth profiles. Here, the experimental set-up is described and the strategy of the energy calibration of MaRPel and the AMSEL-steerers is explained. The resolution and sensitivity of hydrogen depth profiling are presented together with some measured profiles as examples for possible applications of this analytic tool.


*Keywords:* Nuclear reaction analysis; Hydrogen depth distribution; γ-Ray spectroscopy; Hydrogen detection sensitivity; Accelerator calibration

## 1. Introduction

Only a few analytical methods are available which can determine the depth distribution of small amounts of hydrogen. Besides ERDA and SIMS, the Resonant Nuclear Reaction Analysis (RNRA) is a very sensitive tool, which was used in the present study in two-fold ways: firstly to calibrate the accelerator and secondly to detect H-concentrations below the surface of H-containing samples. The RNRA-method makes use of very sharp resonances (1 eV $\leq \Gamma \leq$10 keV) in the cross section of nuclear reactions, which are tabulated (see for example [1] and references there in). Usually, reactions are used which lead to the emission of high-energy gamma quanta of the final nucleus, being a "fingerprint" for the presence of a certain isotope.

Ions accelerated to the resonance energy $E_R$ will react with nuclei at the target surface. When the beam energy $E_B$ is increased, the ions will be slowed down by the stopping power of the target until they reach the exact resonance energy deeper inside the material. In this way, a depth profile is obtained by counting the gamma yield versus the increasing ion beam energy. The depth $x$ is calculated from the difference $(E_B - E_R)$, divided by the stopping power $dE/dx$ of the target material, which is tabulated for pure elements in [2] and can be calculated for more complex materials with the help of the Bragg-rule [3].

Hydrogen depth profiling is performed by selecting a $^{15}$N beam with an energy higher than 6.385 MeV, the exact resonance energy of the $^{1}$H($^{15}$N, $\alpha\gamma$)$^{12}$C nuclear reaction. This resonance has a narrow width of $\Gamma = 1.868$ keV [4] and the high cross section of $\sigma_{6385} = 1650$ mb. The energy of the emitted gamma quanta is 4439 keV. Using 7.2 MeV, the highest possible energy of $^{15}$N ions at MaRPel, hydrogen can be traced, for example in Ti, up to a depth of 320 nm.

## 2. Experimental

For high-sensitivity hydrogen depth profiling, three different experimental devices are required: (1) an accelerator to provide $^{15}$N-ion with at least the resonance energy, (2)

* Corresponding author. Tel.: +49 551 397 613; fax: +49 551 394 493.
*E-mail address:* muhrmac@gwdg.de (M. Uhrmacher).

0925-8388/$ – see front matter © 2005 Elsevier B.V. All rights reserved.
doi:10.1016/j.jallcom.2004.09.092

AMSEL-steerers to vary this energy fast and easily, and (3) a low-level RNRA gamma detection station. The general MaRPel set-up can be found in [1].

The 3ṀV NEC-Pelletron accelerator MaRPel (Materials Research Pelletron) delivers a stable $^{15}$N ion beam with a current of about 25 mA, produced by the ion source SNICS (Source of Negative Ions by Cesium Sputtering) using a Cu-cathode filled with KC$^{15}$N. A good transmission of 1/15 (target to source beam current) has been reached. The field of a 90 °C analyzing magnet determines the beam energy. Because of the need to vary the beam energy consecutively during RNRA-measurements the hysteresis of the 90 °C – magnet would tremendously limit the speed of data taking and continuous refocusing would be necessary. Therefore, MaRPel includes an automatic hysteresis-free energy scanning device – the AMSEL-steerers (details of the experimental set-up are given in Ref. [5]). The high voltage stabilization of a tandem accelerator (TPS-system) uses a beam position sensing "slit control" system right behind the analyzing magnet. The basic idea of Amsel et al. [6] is to "fool" this stabilization system by deflecting the beam at two points, i.e. at the entrance and the exit of the analyzing magnet, through small angles using electrostatic deflection plates. Fig. 1 schematically displays the operation of the AMSEL-steerers. The solid line corresponds to the ideal beam track at fixed values of energy and magnetic field. A negative potential on the two deflector plates on the left-hand side results in the dot-and-dash line. Following a non-symmetrical path, such ions hit the "high-energy-slit". Automatically, the TPS will decrease the beam energy and the ions will then follow a new symmetrical path through the magnet (dotted line). In zero order the correlation between the applied deflector voltage ($0 \leq U \leq 20$ kV) and the change in the acceleration voltage $\Delta U_{acc}$ [7] is linear.

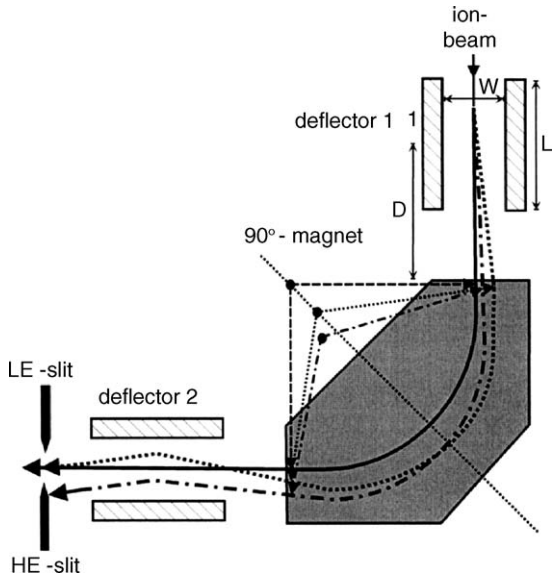


Fig. 1. Different beam trays through the AMSEL-steeres and the 90° analyzing magnet.

The low-level RNRA gamma detection set-up includes a rotatable target holder and a 10 in. × 10 in. NaI-detector, both enclosed in a combination of active and passive radiation shieldings. The outermost shield is the 1 m thick concrete wall of the accelerator hall itself, which reduce the soft component of cosmic and environmental radiation. The next shield is a box made of 30 cm thick old iron (the armoring plates of a Dutch warship build in 1902) which is almost free of radioactive contaminants; its bottom part is "only" 15 cm thick. Inside the iron box, boronated plastic is placed to capture thermal neutrons. In order to suppress penetrating muons generated by the cosmic radiation, 2 cm thick scintillation counters can be mounted on the outer five sides of the iron box, except the bottom side. These scintillators are operated in anticoincidence with the NaI detector and serve as an active shielding; however, they produce a relatively large deadtime of about 20%. A detailed description of the whole low level device (at its first location in the Max-Planck-Institut für Kernphysik, Heidelberg) is given in [8].

## 3. Energy calibration strategy

The most important values for the operation of an accelerator are the exact ion energy $E$ and the energy resolution $\Delta E_{ion}$. The accelerating terminal voltage of MaRPel is measured via a generating voltmeter (GVM) with a poor accuracy ($\Delta U \cong 2$ kV), whereas the magnetic field of the mass separator is controlled via a Hall-probe near the beam trajectory with a high accuracy ($\Delta B \leq 0.1$ mT). Furthermore, the bending radius of the magnet has to be known. It is needed to calculate the magnetic field setting for ions of different mass and energy.

The energy calibration was carried out in four steps. In the first step, the energy of the proton beam was changed by varying both the magnetic field $B$ of the mass separator and the terminal voltage $U_{Terminal}$ of the accelerator, focused on the Faraday cup at the exit of the 90 °C magnet. Using an estimate for the bending radius of the magnet a rough calibration of the GVM was obtained. This allowed the next step: a thin nitrogen layer of a laser-nitrided tantalum sample was analyzed by RNRA. We searched the four resonances in the $^{15}$N(p, αγ)$^{12}$C reaction at $E_R = 898$, 1210, 1640 and 1979 keV [1]. The experimentally obtained energy of these precisely known resonances gave the correction factor for the GVM which allowed to correlate the measured accelerating high voltage $U_{Terminal}$ with the desired beam energy $E_{Beam}$. Fitting the bending power of the mass separator with the now known pairs of $E_{Beam}$ and $B$, the precise value of its bending radius, $r = 0.871(1)$ m, was achieved. With this value being fixed, the corresponding magnetic fields for all ion masses and ion energies can be calculated. The upper part of Fig. 2 shows the experimental data for the magnetic field which is needed to bend the protons or $^{15}$N-ions by 90 °C into the RNRA-beam line. The lines represent the fit of the bending

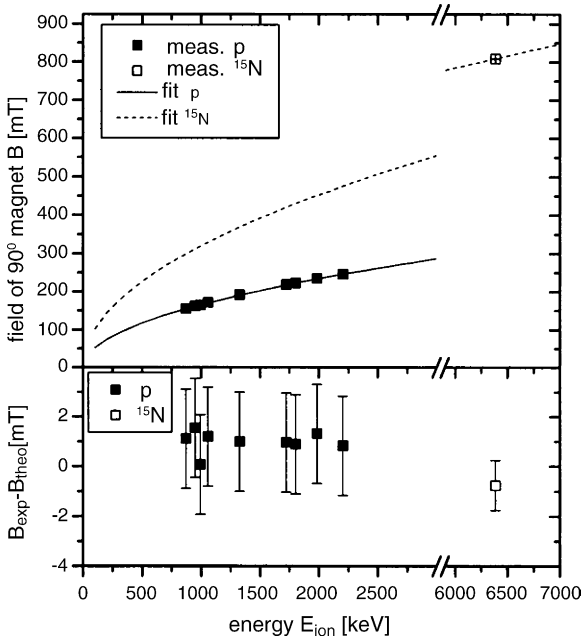


Fig. 2. In the upper part the magnetic field $B$ is given vs. the beam energy, which is necessary to deflect protons or $^{15}$N-ions by 90°. Experimental points are shown together with the theoretical line calculated from the fitted bending radius $r$. The lower part enhances the deviation between calculated and measured values.

radius. The lower part of Fig. 2 gives the deviations of the measured value for $B$ from the calculated ones.

Finally, the "Amsel-steerers" were calibrated in an RNRA experiment with five narrow resonances in the cross section of the $^{27}$Al (p, γ) $^{28}$Si nuclear reaction. Fig. 3 shows the five resonances in the energy region from 730 to 780 keV. The target was a 10 nm thin Al-layer on Ta. The inset of Fig. 3 shows the linear correlation between the resonance energies and the applied deflection voltage $U_{\text{deflector}}$ on the AMSEL steerers. A 1 kV voltage on the deflector plates was found to increases the energy of the proton beam by +20.4 keV. Together with some geometrical corrections this allows a wide variation of the beam energy within one magnet setting: for protons of 1.7 MeV the accessible energy range is 386 keV, for $^{15}$N-ions of 6.4 MeV it is 836 keV.

A lot of different effects give rise to an uncertainty concerning the beam energy $\Delta E_{\text{ion}}$. The ion source already contributes to it. Many factors broaden the beam energy at the high voltage terminal of a tandem, the discontinuous charge delivery, the corona current, the charge-exchange processes of the ion in the stripper-channel and the break-up of molecules, which occurs with the C$^{15}$N molecule. Finally, inhomogeneities of the magnetic field also contribute to the beam-energy broadening. All these effects add up to the final beam width measured by RNRA with the help of a massive Al-target. The reaction $^{27}$Al (p, γ)$^{28}$Si has a very narrow ($\Gamma = 0.05$ keV) [44] resonance at $E_{\text{R}} = 992$ keV. The measured curve is given in Fig. 4. A fit with an error function results in a total width of $\sigma = 0.48(4)$ keV, which gives

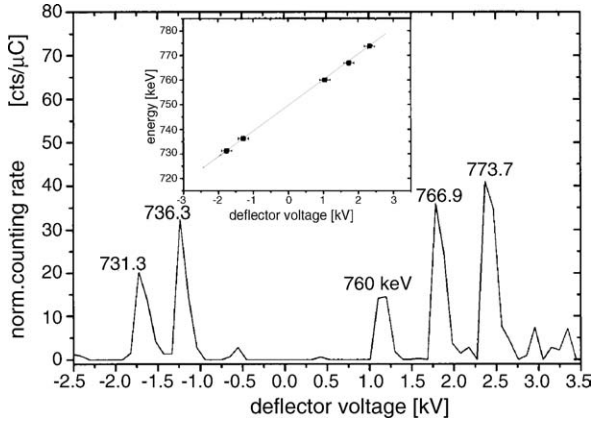


Fig. 3. RNRA spectrum of the (p, γ) reaction in a 10 nm layer Al on Ta. The γ-counting rate is plotted vs. the deflector voltage of the AMSEL-steeres. The inset shows the linear energy calibration.

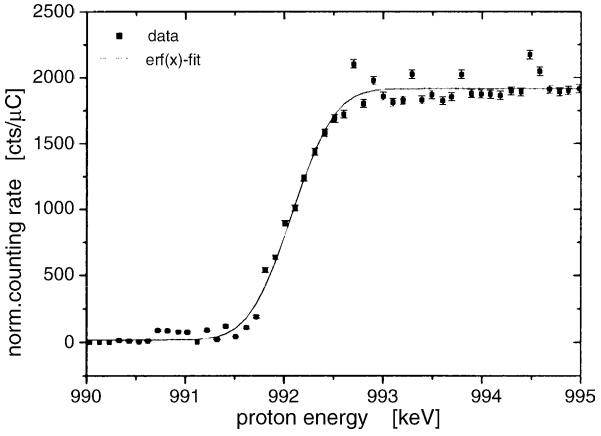


Fig. 4. RNRA spectrum of the (p, γ) reaction on a thick Al-target in the energy range $E_{\text{p}} = 890$–995 keV. The variance $\sigma = 0.48(4)$ keV of the fitted error function gives the upper limit for the energy width of the proton beam.

$\Delta E_{\text{ion}} = (\sigma^2 - \Gamma^2)^{1/2} = 0.48(3)$ keV as the upper limit for the energy width of the proton beam. For the $^{15}$N-beam at 6.4 MeV, we used the width of narrow hydrogen surface peaks to estimate $\Delta E_{\text{ion}} \approx 7(1)$ keV [5]. This value results in a depth resolution of about 2 nm if we apply the tabulated electronic stopping powers of $^{15}$N-ions [2]. Due to the energy straggling in the target this resolution increases from the surface to about 12 nm at a depth of 500 nm.

## 4. Hydrogen sensitivity

In this chapter we will discuss the high sensitivity of RNRA to hydrogen concentrations, and how it can be increased by certain improvements of the detection system and/or by the performance of the experiments. The sensitivity limit ($c_{\text{min}}$ = the minimal concentration, that can be detected) can be found from the statistical error of the normalized gamma reaction yield $Y_{\text{reac}} = (Y_{\text{m}} - Y_{\text{bg}})/it$. Here,

$Y_m$ is the measured yield and $Y_{bg}$ the background yield; $i$ is the ion beam current and $t$ the measuring time. The corresponding counting rates are defined by $\frac{dY_{reac}}{dt} = \dot{Y}_{reac}$ and $\frac{dY_{bg}}{dt} = \dot{Y}_{bg}$.

As shown in detail in [7], the minimal concentration can be calculated when $\dot{Y}_{reac} \ll \dot{Y}_{bg}$:

$$c_{min} = \frac{\dot{Y}_{reac}}{\text{const} \times i} = \frac{1}{\text{const} \times i} \sqrt[3]{\left(2\dot{Y}_{bg}^2 / \left(\frac{\Delta Y_{reac}}{Y_{reac}}\right)^2 \times t\right)} \quad (1)$$

This formula demonstrates that an increase in the ion beam current has the biggest influence on $c_{min}$: one order of magnitude pushes $c_{min}$ down by a factor of 10. Unfortunately, there are limits due to the ion source itself, the optics of the beam line and the thermal stability of the target. In our set-up, the maximum current on the target is about 1.5 μA swept over 1 cm$^2$. The low level measuring set-up is especially designed to decrease the background rate, as has been described before. Here, a factor of 10 leads to a reduction of $c_{min}$ by 4.64. An increase of the data taking time is less important. Here one gains only a factor of 2.15 by increasing the measuring time by a factor of 10. As an example, we give here $c_{min}$ for H in Si. If we assume a maximal relative error $\Delta_{reac}/Y_{reac} = 0.5$ and take as the typical values $\dot{Y}_{bg} = 0.98$ cts/s, const = 21.126 cts/(μC at.%H in Si), $i = 0.5$ μA and $t = 72$ s, $c_{min}$(H) is calculated to be 450 atppm. This value is clearly larger than the previous Heidelberg result of $c_H = 80$ atppm [9], but in these experiments a measuring time of $t = 1000$ s was used.

To demonstrate the wide range of hydrogen concentrations which can be analyzed by this technique in Figs. 5 and 6 depth profiles are shown which strongly differ in their H concentration. In both cases the samples were loaded with H by laser hydriding [10–12]. Fig. 5 shows Ti-samples that have been irradiated with 16, 64 or 256 laser pulses at a fixed fluence of 4 J/cm$^2$ and the given ambient pressure of hydrogen from 0.5 to 3 bar. Under nearly all conditions the H-concentration increases to a mean saturation value of 47 at.%. The limit of 370 nm reflects the maximum depth which can be analyzed with $^{15}$N-ions at MaRPel. As shown in [10,12], this laser treatment leads to the formation of the $TiH_2$ phase. Fig. 6 shows a low H-concentration example, which was obtained after laser-hydriding of a Si sample which has been amorphised by Xe-bombardment prior to the laser hydriding process. The $H_2$ pressure was 2 bar for all samples, the respective laser fluences are given in the figure. All recorded depth profiles show the presence of the well known hydrogen surface peak with a maximum concentration of about 2.3 at.%. However, when applying the 16 pulses with a fluence of 1 J/cm$^2$ we find in addition an increased H-concentration with a maximum of 0.7 at.% H around a depth of 40 nm [10,12].

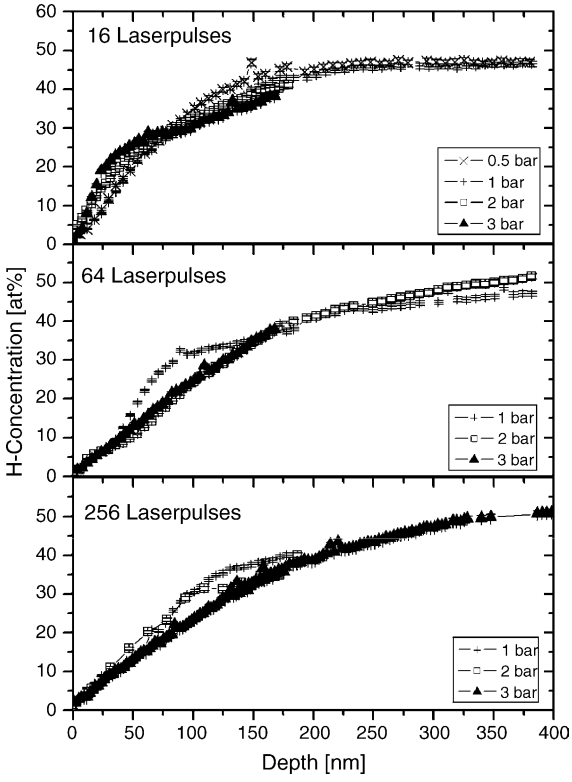


Fig. 5. Hydrogen depth profiles from Ti-samples, which have been laser-hydrided with a fluence of 4 J/cm$^2$ at the given $H_2$-pressure and number of laser pulses.

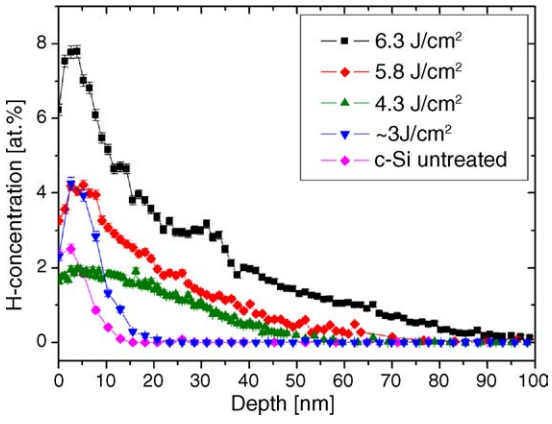


Fig. 6. Hydrogen depth profiles from Si-samples, amorphized by Xe-ions before, after laser-hydriding with 16 pulses at a $H_2$-pressure of 2 bar.

## 5. Conclusions

It has been shown that MaRPel and the low-level RNRA set-up is capable of high sensitivity H depth profiling. Using short measuring times of about 1 min/energy the sensitivity limit is at 0.045 at.% for the detection of H in Si. After calibrating the AMSEL-steerers, also computer-controlled measurements are also possible which allow a fast hydrogen depth profiling in a range of about 400 nm in Si samples.

Within this range the depth resolution increases from 2 to 10 nm.

## Acknowledgements

The authors are very grateful to the Max-Planck-Institut für Kernphysik, Heidelberg, for the donation of the MaRPel accelerator.

## References

[1] M. Schwickert, F. Harbsmeier, H. Schebela, M. Uhrmacher, E. Carpene, P. Schaaf, K.-P. Lieb, Surf. Coat. Technol. 151/152 (2002) 222.
[2] J.F. Ziegler, J.P. Biersack, U. Littmark, The Stopping and Range of Ions in Solids, vol. 1, Pergamon Press, New York, 1999.
[3] W.H. Bragg, R. Kleeman, Philos. Mag. 10 (1905) 318.
[4] A. Schardt, W.A. Fowler, C.C. Lauritsen, Phys. Rev. 86 (1952) 527.
[5] M. Zinke-Allmang, V. Kössler, S. Kalbitzer, Nucl. Instr. Meth. B15 (1986) 563.
[6] G. Amsel, E. d'Artemare, E. Girard, Nucl. Instr. Meth. 205 (1983) 5.
[7] M. Schwickert, Doctoral Thesis, Universität Göttingen, 2002.
[8] H. Damjantschitsch, et al., Nucl. Instr. Meth. 218 (1983) 129.
[9] H. Becker, Diploma Thesis, MPI-Kernphysik, Heidelberg, 1991.
[10] M. Schwickert, E. Carpene, M. Uhrmacher, P. Schaaf, K.P. Lieb, Appl. Phys. A 77 (2003) 793.
[11] M. Schwickert, E. Carpene, K.P. Lieb, M. Uhrmacher, P. Schaaf, Physica Scripta T108 (2004) 113.
[12] M. Schwickert, E. Carpene, K.P. Lieb, M. Uhrmacher, P. Schaaf, Appl. Phys. Lett. 84 (2004) 5231.